J Indian Acad Wood Sci (June 2018) 15(1):68–79
https://doi.org/10.1007/s13196-018-0210-9

ORIGINAL ARTICLE

Morphological, chemical, and thermal characteristics of chitosan nanocomposite films reinforced with steam-exploded microfibrillated cellulose

Achmad Solikhin[1] · Bambang Hermawan[2] · Eti Artiningsih Octaviani[3] · Dita Sari Prabuningrum[1] · Nurmadina[1] · Imam Gazali[1] · Silvia Uthari Nuzaverra Mayang Mangurai[1] · Kazushige Murayama[4] · Sahriyanti Saad[4]

Received: 27 May 2017 / Accepted: 28 March 2018 / Published online: 3 April 2018

Abstract The objective of the study was to investigate and analyze the morphological, chemical, and thermal properties of chitosan nanocomposite films reinforced with microfibrillated cellulose (MFC). MFC, which was isolated via steam explosion assited with alkaline treatment, produced a diameter size average of about 50 nm with self-aggregated ball-like shapes. Obtained chitosan/MFC nanocomposite films had a varied thickness average and moisture content in the range from 3.70 to 13.34%. Chitosan films had a good UV prevention without sacrificing transparency nature. The reinforcement of MFC 0.5–2.5% and MFC 5–10% in the films induced irreversible self-aggregation with a size average of about 0.5 and 10 µm, respectively. Carbon and oxygen elementals varied whereas nitrogen slightly decreased along with MFC incorporation. The addition of MFC into chitosan films noticeably shifted FT-IR wavenumber and intensity because of chemical interaction between chitosan and MFC functional groups. MFC enhanced the thermal stabilities of chitosan films due to high remnant weight of the films after thermal decomposition although MFC accelerated the decomposition and degradation of the films. The inclusion of MFC into chitosan polymer did not show anti-bacterial properties against *Escherichia coli* due to no clear zone of inhibition and no zone of inhibition indices around the tested films.

Keywords Nanocomposite films · Chitosan · Microfibrillated cellulose · Steam explosion

✉ Achmad Solikhin
achmad.solikhin1993@gmail.com

[1] Department of Forest Products, Faculty of Forestry, Bogor Agricultural University, Bogor, Indonesia

[2] Department of Physics, Faculty of Mathematics and Natural Sciences, Bogor Agricultural University, Bogor, Indonesia

[3] Department of Silviculture, Faculty of Forestry, Bogor Agricultural University, Bogor, Indonesia

[4] Department of Environment and Forest Resources Science, Faculty of Agriculture, Shizuoka University, Shizuoka, Japan

Introduction

Nowdays, the fabrication and application of nanotechnology have been a mesmerizing concern for researchers and composite-based industries. Besides bacterial nanocellulose and cellulose nanocrystals, microfibrillated cellulose (MFC) is one of the types of cellulose nanofiber, which has been used for wide range of applications, such as: packaging, automotive, electronics, sensor application, and biomedical tools (Kumar et al. 2014). MFC has excellent properties, such as sustainable, biodegradable, low density, relatively reactive surface, high aspect ratio, and high strength (Qi et al. 2013; Zhou et al. 2015). From these properties, MFC has the potential as an alternative for synthetic reinforcement agent for nanocomposite films. Previous studies of MFC utilization for a reinfocing agent to nanocomposite films were reported, such as MFC-graphite nanocomposite films for battery electrode (Jabbour et al. 2010), MFC/chitosan-benzalkonium chloride for enhancing alginate films (Liu et al. 2013), and MFC/polypyrrole/silver nanoparticles for hybrid aerogels (Zhou et al. 2015).

MFC can be isolated via mechanical disintegrations of cellulose fibers assisted with chemical treatments with aim to reduce high energy consumption. High pressure homogenization (Siqueira et al. 2010; Li et al. 2012), grinding (Osong 2014), and cryocrushing methods (Herzele

et al. 2015) are the examples of mechanical methods used to synthesize MFC. The resultant fibers have a diameter average in the range from 10 to 100 nm and aspect ratios of about 50–100 nm (Tingaut et al. 2012) as well as the length in several micrometers (Chang and Wang 2013). Another method used to isolate MFC is by means of steam explosion assisted with chemical treatment. Cherian et al. (2012) and Deepa et al. (2011) stated that steam explosion coupled with acid treatment effectively isolated cellulose nanofibrils of pineapple leaf and banana fibers, respectively. The technique reduced the microfibers size of about 5 μm to less than 50 nm with interwoven individual fibrils-like structure.

In manufacturing of nanocomposite films, considering the types of matrix is verily indispensable due to the imparted nanocomposite properties. Edible, affordable, compatible, biodegradable, anti-bacteria and anti-fungi, and excellent mechanical characteristics (Azeredo et al. 2010; Hafdani and Sadhegenia 2011; Charernsriwilaiwat et al. 2012; Pavaloiu et al. 2014; Park et al. 2015; Mahmoudi et al. 2016) are necesserily expected for food packaging nanocomposite films. Chitosan is one of the biopolymers, consisting of β-(1,4)-2-amino-2-deoxy-D-glucopyranose extracted from chitin by deacetylation in the presence of alkali (Pavaloiu et al. 2014). Chitin can be extracted from insects, mollusks, and shellfish (shrimp, lobster, and crabs) (Paipitak et al. 2011). This biopolymer has the potential as a matrix due to excellent characteristics, such as bioactive, biocompatibe, biodegradabe, soluble in an aqueous solution, good ability to form complexes, and non-toxic for humans (Lewandowska 2015). This biopolymer is not only for biomedical application but also for food packaging because of producing clean, tough, and flexible films with good oxygen barrier (Azeredo et al. 2010), low cost, abundant availability, and excellent film forming capability (Bajpai et al. 2015).

Studies about nanocomposite made from chitosan/cellulose nanofibers have been carried out by several researchers, such as chitosan/cellulose nanocrystal (Mesquita et al. 2012; Celebi and Kurt 2015; Zeid et al. 2015), chitosan/carbon nanotube (Song et al. 2015; Postnova et al. 2015), chitosan/nanocellulose (Dehnad et al. 2015), and chitosan/nanofibrillated cellulose (Fernandes et al. 2010; Hassan et al. 2011). However, the utilization of chitosan/MFC blend for nanocomposite films has been less-studied (Hassan et al. 2011; Liu et al. 2013, 2014; Balan et al. 2015), particularly chitosan polymer reinforced with oil palm empty fruit bunch fibers MFC. In this study, OPEFB fibers were utilized for producing MFC due to its superior properties, such as renewable, abundant, and biodegradable. MFC has also excellent mechanical properties generated by high surface reactivity and aspect ratio, leading to form percolation network with MFC and other polymers. Besides MFC, OPEFB fibers had been utilized for lignocellulose potential sources for cellulose nanofibers (Haafiz et al. 2013; Goh et al. 2013; Romainor et al. 2014).

From the above, the fabrication of chitosan nanocomposite films reinforced with MFC is very imperative to be studied because of its potential as an edible transparent food packaging. In this study, the isolation of MFC was undertaken by an hour continuous steam explosion method coupled with alkaline treatment (Solikhin et al. 2017). In addition, chitosan nanocomposite films reinforced with an hour steam-exploded—MFC will be characterized by using SEM, EDS, FTIR, TGA, DTA, and anti-bacteria properties. The objective of the study was to investigate and analyze the morphological, chemical, and thermal properties of chitosan/MFC nanocomposite films.

Experiment

Materials

Microfibrillated cellulose was extracted from oil palm empty fruit bunch fibers (OPEFB) by means of chemo-mechanical method. The fibers were taken from PT Perkebunan Nusantara VIII, Bogor, Indonesia. Chitosan was supplied from Biotech Surindo with an acetylation degree of 85.13% (w/w) and particle size of 20–30 mesh. Analytical grade of chemicals consisted of 98% acetic acid (CH_3COOH), 30% hydrogen peroxide (H_2O_2), 98% formic acid (CHOOH), and sodium hydroxide (NaOH) that were supplied from Merck KGaA, 64271 Darmstadt, Germany. Gram positive bacteria, *Escherichia coli*, were brought from IPB Culture Center, Indonesia, used to anti-bacterial test.

Isolation of microfibrillated cellulose

The isolation of MFC referred to Solikhin et al. (2017), and was conducted by using Ultra-turrax homogenization and ultrasonication assisted with chemical pretreatments. OPEFB vascular bundles were disk milled via a modified dry-disk milling for 30 min, and obtained OPEFB microfibers were sieved with a 100–200 mesh filter. About 20 g of the microfibers were subsequently extracted with a soxhletation method in 300 mL of ethanol: acetone at a ratio 1:2 (v/v %) for 7–8 h. The fibers were continued to be immersed in the mixture of 5% NaOH and 5% H_2O_2, and were autoclaved at 121 °C under a pressure of 1.5 bar for 1 h. The autoclave process assisted with these chemicals was used to autohydrolize silica, delignify lignin, and remove hemicellulose imparted in the fibers.

To clean turbid slurry, acquired fibers were washed several times with distillated water. Clear fibers were

immersed in 10% H_2O_2 and 20% CHOOH solution at a ratio of 1:1. The mixture was heated in a shaking bath, and the shaking machine was set at 60 °C with a rate of 90 rpm for 90 min. The fibers were then rewashed with distillated water, and were continued with resuspending in a mixture of 5% H_2O_2 and 5% NaOH. The mixture was continuously steam-exploded by using an autoclave at 121 °C under a pressure of 1.5 bar for 1 h. The obtained cellulose was rewashed with distillated water for several times until clear suspension was obtained. Finally, the suspension was ultasonicated with an ultrasonication (Ultrasonic Processor Cole Parmer Instrument, USA) in an ice water bath for 25 min with an amplitude of 40%, a power of 130 Watt, and a frequency of 20 kH.

Fabrication of chitosan/MFC nanocomposite films

About 3 wt% chitosan was dissolved in 1% CH_3COOH, and was mechanical-stirred at room temperature with a stirring rate of 150 rpm for 5 h. Different MFC contents (0, 0.5, 2.5, 5, 7.5, and 10 wt%) were mixed with chitosan solution. The mixture of chitosan and MFC was mechanically stirred at 200 rpm for 3 h at a temperature of 35 °C. The mixture was subsequently solvent-casted in a polypropylene plate for 3 days to evaporate water. To obtain good nanocomposite films, the films were conventionally ovened at a temperature of 45 °C for 24 h. Obtained films were named based on MFC concentration: neat or pure chitosan, chitosan/MFC 0.5%, chitosan/MFC 2.5%, chitosan/MFC 5%, chitosan/MFC 7.5%, and chitosan/MFC 10%.

Characterizations

Transmission electron microspcope

A drop of MFC suspension was analyzed by means of a transmission electron microscope (JOEL, Japan) to investigate the precise nanosize of MFC. Prior to the test, the drop was allowed to dry on a-400 mesh carbon-coated copper grid without uranyl acetate staining. The dried fibers were coated with a sputtering coater (JEC 560, JEOL Japan).

Film thickness and density

A digital micrometer with an accuracy of 0.001 mm was utilized to measure film thickness. The measurement was conducted for 8 different random position of the film. Moisture content of chitosan/MFC films was measured by placing 3 cm × 1 cm films at 110 °C to reach constant weight of the films. The moisture content of the films was calculated on the basis of wet weight.

UV–Vis spectrophotometry (UV–Vis)

Optical properties of chitosan/MFC nanocomposite films were investigated using a UV–vis spectrophotometer (USB4000 Miniature Fiber Optic Spectrometer, Ocean Optics Inc., USA). A wavelength range in the range from 200 to 800 nm was used for analysis.

Scanning electron microscope (SEM)

External surface morphology of chitosan/MFC nanocomposite films was investigated with a scanning electron microscope (JSM-6510, Japan). The analysis was run at 15 kV with a magnification of 190 × (100 μm). Before the test, the samples were ultra-thin coated with platinum via an Autofiner Coater (JEOL JEC-300 FC).

Energy-dispersive X-ray spectroscopy (EDX)

EDX analysis (JEOL EDS, Japan) was performed to investigate the elemental components of chitosan/MFC nanocomposite films. The analysis was undertaken at 10.0 kV accumulation voltage and 0–20 keV energy range. A ZAF method was used for detecting the elements.

Fourir transmission-infrared spectroscopy (FT-IR)

The chemical changes of functional reactive groups in chitosan/MFC nanocomposite films were determined by using a fourier transform-infrared spectroscopy (MB3000, ABB Canada). It was run in the wavenumber range between 4000 and 370 cm^{-1} with a ratio of KBr: chitosan/MFC film of 1:1.

Thermogravimetry/differential thermal analyzer (TG/DTA)

A thermogravimetry analyzer coupled with a differential thermal analysis (Rigaku, Japan) was utilized to analyze thermal properties of chitosan/MFC nanocomposite films. The analysis was run in temperature range from 40 to 400 °C under a gas flux rate of 4 °C/min. Prior the test, about 2.4 mg of the tested films was entered into Al crimp pan with Al_2O_3 as a reference.

Anti-bacterial property

An agar diffusion test was used to investigate the anti-bacteria property of the films againts *E. coli*. Culture medium and petri disk were autoclaved for 30 min,

121 °C, and 1.5 bar. The films (a diameter of 5 mm) were incubated for 2 days at 37 °C.

Result and discussion

Transmission electron microscope

Figure 1 shows a precise nanosize of MFC suspension. MFC had a diameter size of below 50 nm with grape-like shapes that indicated the presence of individual MFC aggregation. The aggregation is due to strong hydrogen bonds and weak Van der Waals forces with reversible nature. Due to the nature, the aggregation is able to be prevented by means of surface modifications (acetylation, esterification, and succynilation) or mechanical disintegrations (ultrasonication, homogenization, and grinding) (Wu et al. 2014). The modifications are able to improve miscibility and interfacial adhesion between MFC and chitosan matrix. In addition, ultrasonication and homogenizer can also breakdown the aggregation via sonochemistry cavitation and mechanical defibrillation. After SAED (Selected Area Electron Diffraction) analysis, MFC was comprised by amorphous and crystalline domain (data were not shown). It indicated that chemical treatment and ultrasonication could not totally loss the amorphous region in MFC.

Film thickness and moisture content

Film thickness and moisture content are two important parameters, which affect physical properties of nanocomposite films. All the films had varied thickness average. The difference was due to the different MFC concentration used to a reinforcing agent in chitosan polymer. In addition, aggregated MFC can induce some protrusions in the external surfaces of the films. The moisture content of the films was in the range of 3.70–13.34%. The remnant of moisture content was in form of bound water that occured because of chemical interaction between hydroxyl groups of chitosan and MFC. In addition, absorbed water could be another reason for the presence of water in the films. However, the moisture content will play role as a plasticizing agent that can be further detected by using a thermal stability analyzer.

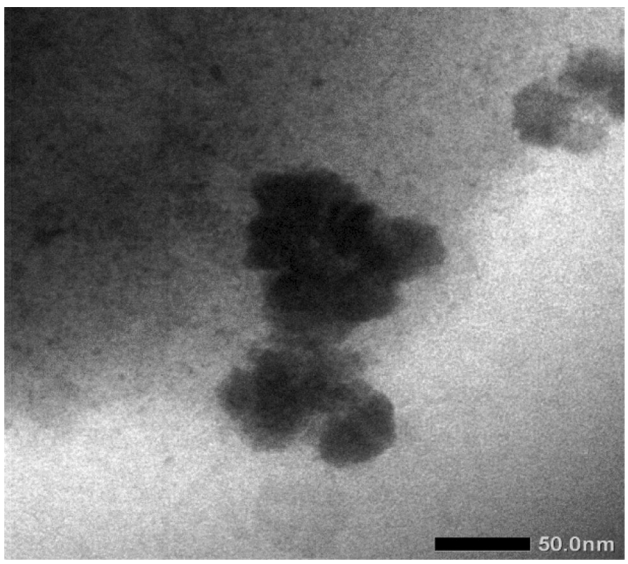

Fig. 1 Graph of MFC suspension with a magnification of 50 nm

Ultraviolet visible spectrophotometry

Figure 2 shows the optical properties of chitosan/MFC nanocomposite films. All the chitosan/MFC nanocomposite films had good transparency in MFC 0.5–5% (transmittance above 50%), and had bad transparency (transmittance below 50%) in MFC 10%. The good transparency is due to well-dispersed MFC into chitosan polymer without some aggregations. In reverse, the bad transperency of chitosan/MFC 10% films is due to the aggregation and non-homogeneity of MFC in the films, inducing light scattering and absorption from chitosan/MFC interface (Wu et al. 2014). In addition, good transparency of the films will allow light to be transmitted because MFC has smaller dimension (nano-sized particles) (Solikhin et al. 2017).

The transmittances of neat chitosan and chitosan/MFC films at wavelength of 380, 400, 500, 600, and 700 nm are tabulated in Table 1. Neat chitosan film had a transmittance percentage of about 95.13% at an ultraviolet wavelength of 380 nm and 85.66% at a visible wavelength of 400 nm. The transmittances of chitosan/MFC films decreased along with the increase in MFC concentration. As compared with chitosan/MFC films, the transmittance

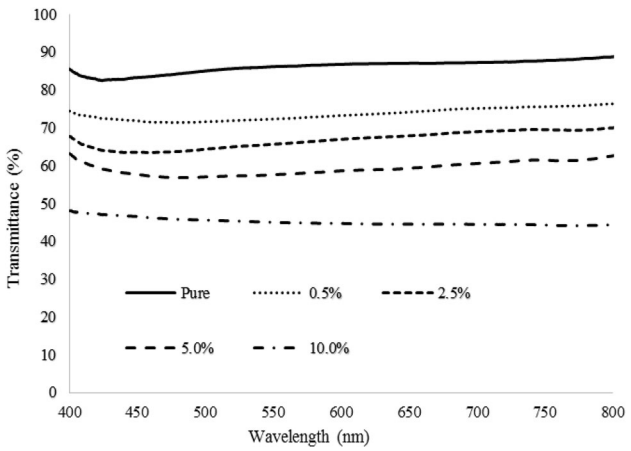

Fig. 2 Transparency properties of neat chitosan film and chitosan/MFC nanocomposite films at 400–800 nm

Table 1 Transmittance of neat chitosan and chitosan/MFC composite films at 400, 500, 600, 700, and 800 nm

Wavelength (nm)	Composite film				
	Neat chitosan	Chitosan/MFC 0.5%	Chitosan/MFC 2.5%	Chitosan/MFC 5%	Chitosan/MFC 10%
380	93.15	78.03	73.72	70.08	49.93
400	85.55	74.33	67.68	63.05	48.04
500	85.00	71.55	64.27	57.06	45.52
600	86.77	73.19	66.90	58.63	44.65
700	87.24	75.05	68.90	60.51	44.39
800	88.75	76.28	69.94	62.50	44.25

percentage of neat chitosan film at 380, 400, 500, 600, 700, and 800 nm was about 93.15, 85.55, 85.00, 86.77, 87.24, and 88.75%, respectively. Neat chitosan film had lower prevention for ultraviolet wavelength transmission than that of chitosan/MFC films. Low ultraviolet transmission and good transparency are desirable for food and packaging plastic application. The incorporation of MFC into chitosan polymer decreased the transmittance percentage with transmittances of about 73.58% (chitosan/MFC 0.5%), 66.83% (chitosan/MFC 2.5%), 59.25% (chitosan/MFC 5%), and 45.01% (chitosan/MFC 10%). The lowest transmittance was in chitosan/MFC 10% films due to non-homogenous distribution and not good miscibility between chitosan and MFC.

Scanning electron microscopy

External surfaces of chitosan/MFC nanocomposite films can be shown in Fig. 3. Neat chitosan composite film had smooth, regular, and even external surfaces with some clear spots, appearing in the surfaces. The spots were due to non-dissolved chitosan biopolymer in acetic acid solvent. The increase in MFC concentration induced irregular, unsmooth, and uneven external surfaces of chitosan/MFC nanocomposite films. It was presumably due to non-homogenous distribution of MFC in the films. The phenomenon was clearly shown by the presence of some white-colored spots or protrusions with an average size of about 0.5 in MFC 0.5–2.5%. The aggerated spots were also easily to be found with an average size above 0.5 μm in MFC 5–10%.

However, chitosan/MFC nanocomposite films reinforced with MFC 0.5–2.5% had better homogenous distribution of MFC than these reinforced with MFC 5–7.5%. That proposition indicates the good compatibility between chitosan and MFC. The aggregated spots are known as irreversible self-aggregations, occuring in the external surfaces of the films due to non-homogenous dispersion of MFC in chitosan polymer. This condition was similar with the prior studies (Fernandes et al. 2010; Bajpai et al. 2015; Song et al. 2015; Dehnad et al. 2015). The aggregations of MFC can lower mechanical strength of the nanocomposite films so that MFC surface modifications, such as solvent exchanges and mechanical defibrillations, can be utilized to prevent it.

Energy dispersive X-ray

Energy dispersive X-ray was utilized to investigate the chemical elements of chitosan/MFC nanocomposites films (Fig. 4). The dominant elements of the films are tabulated in Table 2. Neat chitosan films had carbon of 33.36%, oxygen of 29.92%, and nitrogen of 36.72% whereas the incorporation of MFC shifted the percentage of these elements. The shift was slightly different, and no dramatic change was identified for C (33.04–33.60%), O (29.92–30.63%), and N (36.15–36.72%). However, the reinforcement of MFC into chitosan polymer slightly decreased the element of nitrogen over neat chitosan film. It is because nitrogen was reacted with H or O to create inter- and intra-molecular hydrogen bonds. Carbon and oxygen were from MFC and chitosan whereas nitrogen was from chitosan biopolymer. In addition, carbon and oxygen were easily observed as the major component of hemicellulose and lignin that were still deposited in the MFC. It indicates that these elementals are dominant for both cellulose and chitosan.

Fourier transmission-infrared spectroscopy

Figure 5 highlights the FT-IR spectra of chitosan/MFC nanocomposite films. As compared with neat chitosan film, the reinforcement of MFC into chitosan polymer noticeably shifted FT-IR spectra. The shift was observed in wavelength and intensity. The phenomenon occurred because of chemical interaction between chitosan and MFC functional groups. Neat chitosan film had a broad peak in the range from 3500 to 3000 cm^{-1} that indicated O–H of

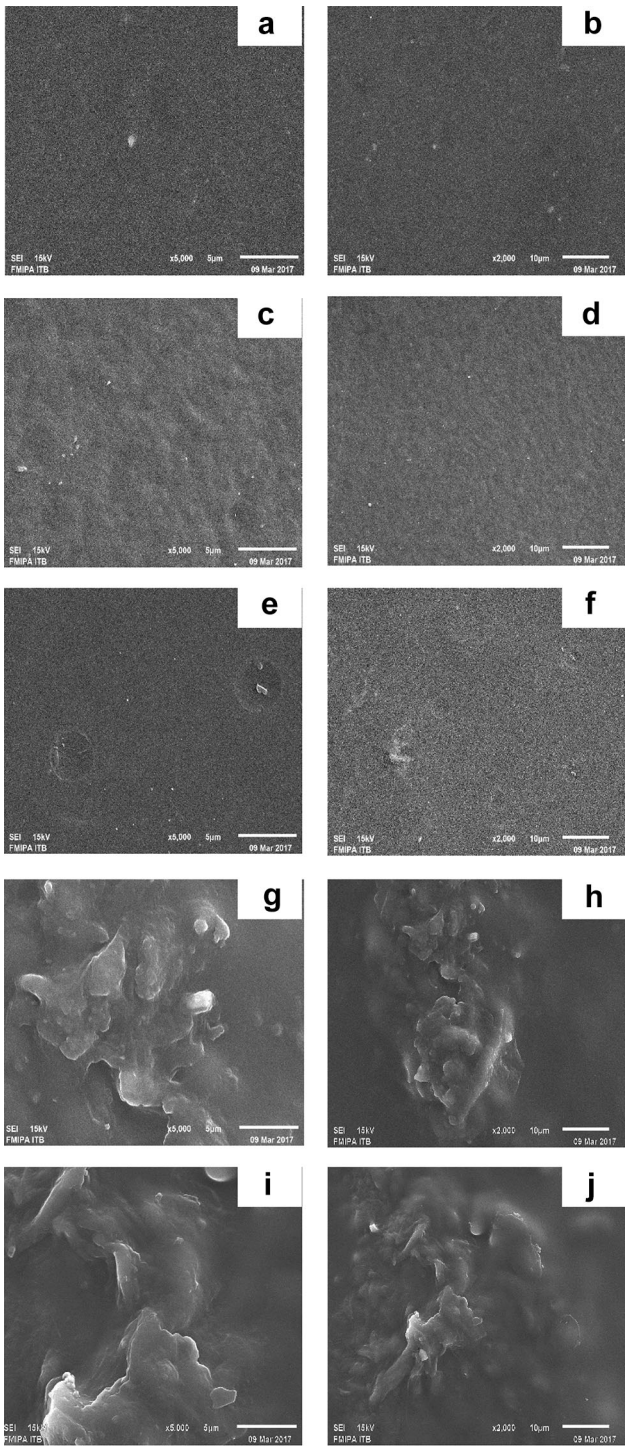

Fig. 3 External surfaces micrographs of nanocomposite films at magnification of 5000× and 2000× **a**, **b** pure chitosan, **c**, **d** chitosan/MFC 0.5%, **e**, **f** chitosan/MFC 2.5%, **g**, **h** chitosan/MFC 5%, and **i**, **j** chitosan/MFC 10%

MFC (Solikhin et al. 2017) and N–H streching vibration of chitosan (Fernandes et al. 2010, Solikhin et al. 2018). The broad peak of each nanocomposite film was overlapped with varied intensity and shifted wavenumber. The changes indicate the increase in hydrogen bonds due to the interaction between the hydroxyl groups of MFC and chitosan.

The addition of MFC altered two IR peaks at 2929 and 2881 cm^{-1} of chitosan films, corresponding to symmetric and asymmetric C–H vibrations of MFC, respectively (Liu et al. 2013, Lewandowska 2015). Peaks around 1610 and 1556 cm^{-1} were attributable to –CONH–stretching vibration in chitosan and C–C stretching vibration of MFC, respectively (Gulmen et al. 2015, Ostadhossein et al. 2015). These peaks had varied intensity that indicated the reaction between MFC and chitosan functional groups (Celebi and Kurt 2015). Two representatives of C–H symetric deformation and bending vibration were identified at transmittance peaks at 1460 and 1350 cm^{-1} (Santos et al. 2014), respectively. These peaks appeared in all tested films. Two unique peaks at 1114 and 1014 cm^{-1} in chitosan/MFC nanocomposite films indicated C–O stretching of cellulose (Lewandowska 2015). However, these peaks slightly disappeared in chitosan/MFC nanocomposite films because of chemical interaction between chitosan and MFC. Other transmittance bands, 895 and 669 cm^{-1}, were assigned to C–C stretching of chitosan and chitosan crystallinization (Chen et al. 2007, Tome et al. 2013). The intensity of chitosan films was obviously stronger with the reinforcement of MFC than that without MFC addition due to the interaction between MFC and chitosan.

Thermogravimetry analysis

Thermogravimetry analysis of neat chitosan film and chitosan/MFC nanocomposite films are presented in Fig. 6. From the Figure, it is clear that there are two steps of thermal decomposition of the films. These steps comprised water evaporation and structural degradation for both chitosan and MFC. By reinfocing MFC into chitosan polymer, a noticeable change of thermal stability and weight loss of chitosan/MFC films was noticed. Neat chitosan film began to evaporate physically absorbed in temperature range from 20 to 114 °C with 5% weight loss percentage. On the other hand, the evaporation process of chitosan/MFC films was around 20–120 °C with 3% weight loss percentage (Fernandes et al. 2010, Lewandowska 2015). Chitosan/MFC nanocomposite films had lower weight loss that neat chitosan film because MFC can be a blocking agent for water. However, the strongly chemical bound water between chitosan and MFC continued to be released above 120–190 °C. There was the decrease in weight loss of chitosan polymer reinforced with MFC at 5 and 10% because of the influence of chemical bound water that played a role as a plasticizing and swelling agent. The agent improves the movement of chitosan/MFC polymer blends, and decreases the crystallinity of the polymer.

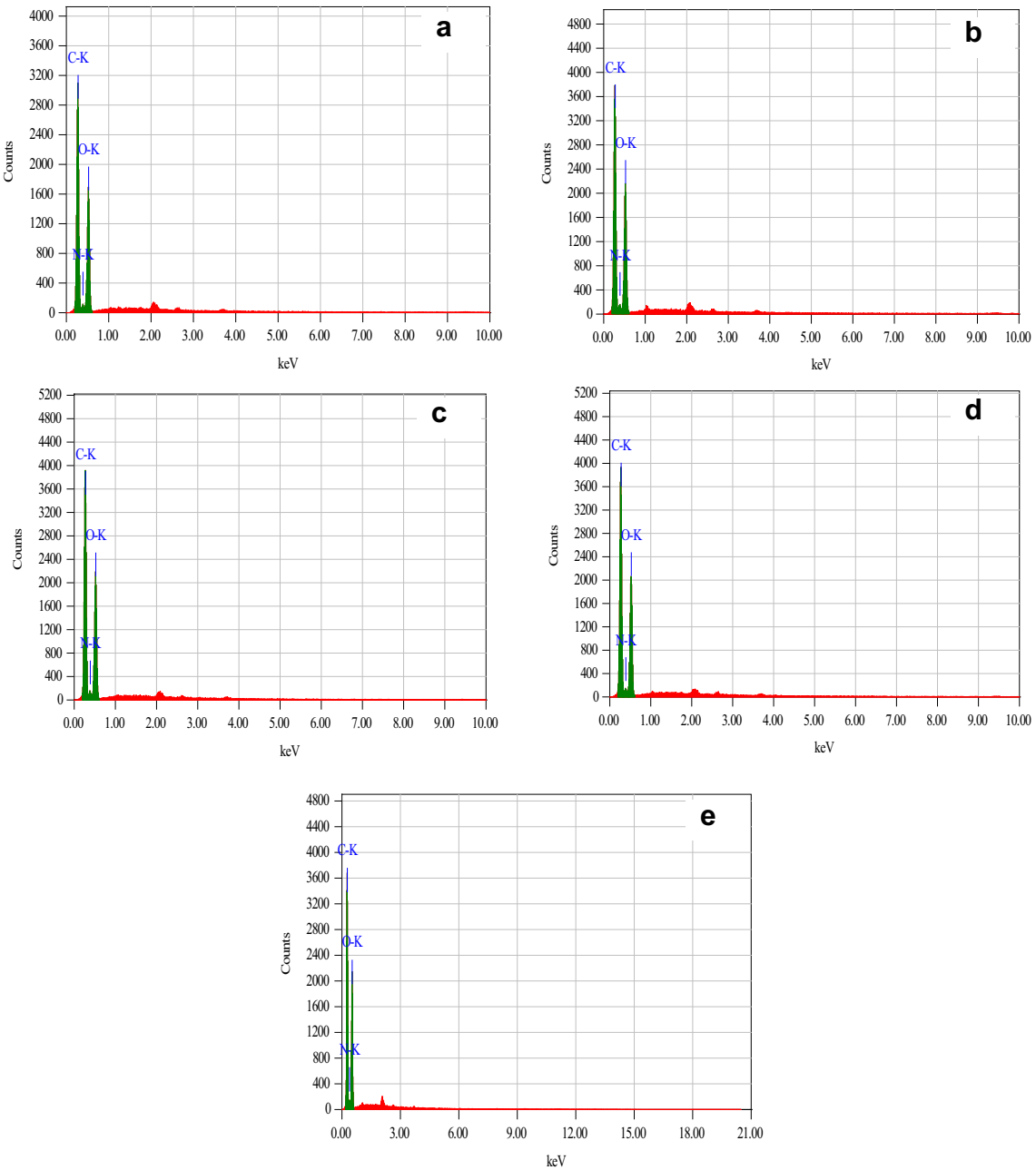

Fig. 4 Energy-dispersive X-ray analysis of chitosan/MFC nanocomposite films: **a** neat, **b** MFC 0.5%, **c** MFC 2.5%, **d** MFC 5% and **e** MFC 10%

A dramatic weight loss around 40% of neat chitosan and 5–10% of chitosan/MFC nanocomposite films was identified in temperature range of around 202–400 and 248–400 °C, respectively. The loss is attributable to structural depolymerization of chitosan polymer backbone chains and the cleavage of glycosidic linkages of cellulose (Fernandes et al. 2010; Bajpai et al. 2015). From the above analysis, it is obvious that MFC enhanced the thermal stabilities of chitosan films through strong hydrogen bonding between MFC and chitosan polymer. The presence of MFC can modify chitosan chain orientation and increase regularity of chitosan matrix, leading to the promotion of crystallization and nucleation process in chitosan matrix. Furthermore, the weight remnant of nanocomposite films after decomposition process was higher than that of neat chitosan film at temperature above 400 °C. In the temperature, final residue is different for each nanocomposite films, attributable to the variance of MFC size and concentration, facilitating the formation of char.

Table 2 Elemental components of neat chitosan and chitosan/MFC composite films

Nanocomposite films	Elementals (%)		
	C	O	N
Neat chitosan	33.36	29.92	36.72
Chitosan/MFC 0.5%	33.60	29.83	36.57
Chitosan/MFC 2.5%	33.38	30.46	36.15
Chitosan/MFC 5%	33.04	30.63	36.34
Chitosan/MFC 10%	33.13	30.57	36.30

Differential thermogravimetry analysis

Figure 7 depicts a differential thermal analysis of neat chitosan film and chitosan/MFC nanocomposite films. In that figure, there are two peaks, which can be used to identify the thermal stability of the films. These peaks are at 253 and 274 °C (neat chitosan), at 238 and 263 °C (chitosan/MFC 0.5%), at 242 and 270 °C (chitosan/MFC 2.5%), at 252 and 264 °C (chitosan/MFC 5%), and at 218 and 260 °C (chitosan/MFC 10%). These temperatures are the initial decomposition and maximum degradation tem-

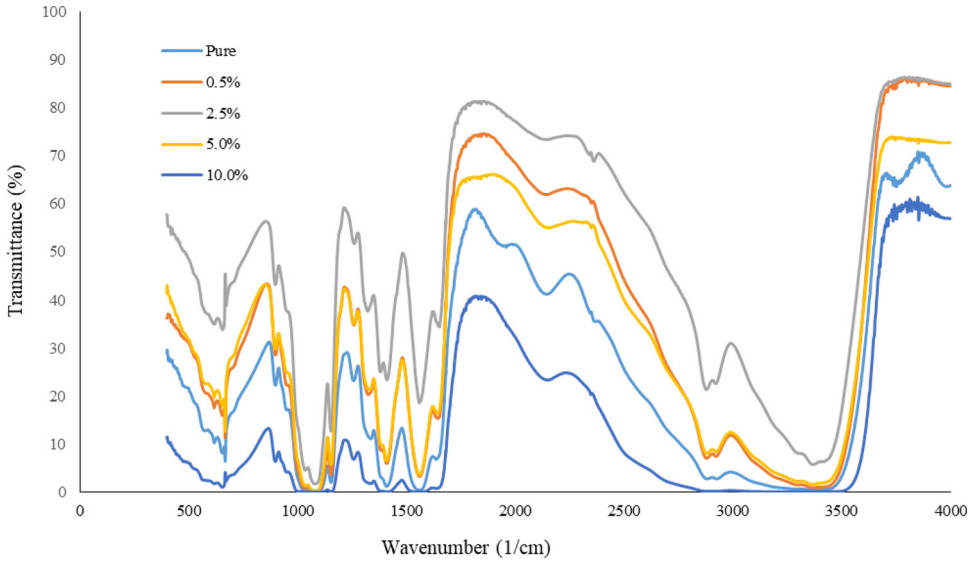

Fig. 5 FT-IR spectra of neat chitosan film and chitosan/MFC nanocomposite films

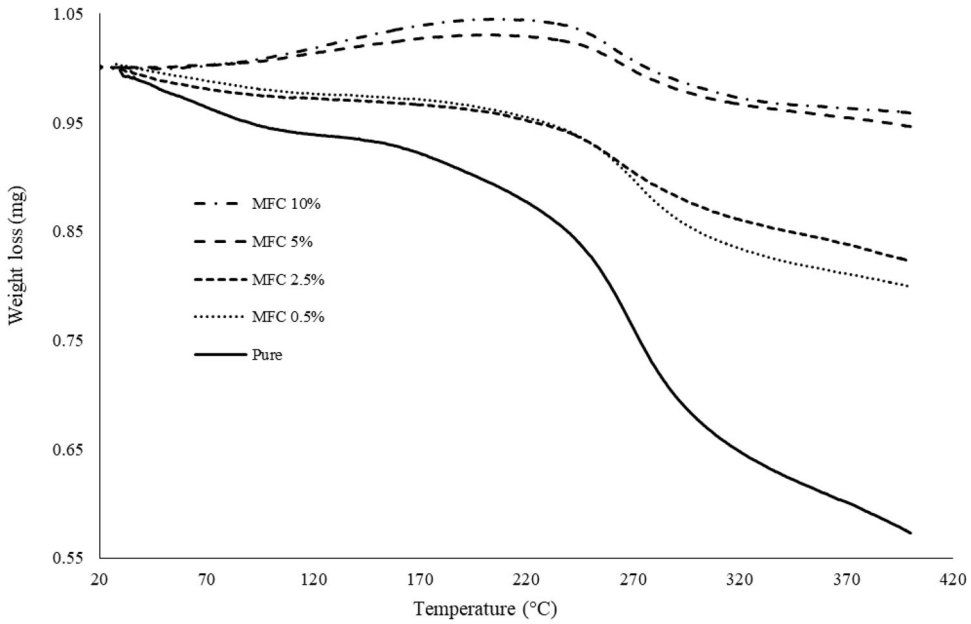

Fig. 6 TGA analysis of pure chitosan film and chitosan/MFC nanocomposite films

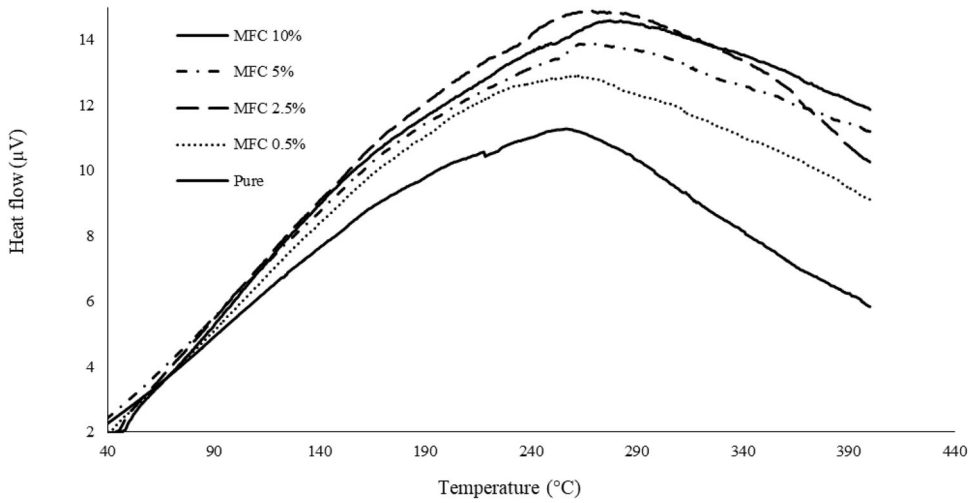

Fig. 7 DTA analysis of pure chitosan film and chitosan/MFC nanocomposite films

perature of the films. While compared with neat chitosan film, the addition of MFC at filler loading of 0.5, 2.5, 5, and 10% decreased the initial decomposition and maximum degradation temperature of chitosan/MFC nanocomposite films. These phenomena were similar with prior studies on chitosan/nanocellulose nanocomposite films (Liu et al. 2013; Solikhin et al. 2018). It is obvious because MFC hampered the decomposition and degradation of the films due to nucleating effects of crystalline of cellulose, inducing the decrease in thermal decomposition (Solikhin et al. 2018).

In addition, a broad endothermic hump had two thermal events, including evaporation or volatilization and degradation of the composite materials. The decomposition and degradation temperature are indicated with the pyrolysis of polysaccharide-like structures of both chitosan and MFC. The process starts with the split of the glycosidic linkages and the decomposition of the six membered-ring moiety (Caloch et al. 2016).

Anti-bacterial properties

Anti-bacterial properties of neat chitosan and chitosan/MFC composite films againts *E. coli* is shown in Fig. 8. For all tested composite films, there was no zone of inhibition (ZOI) and zone of inhibition index (ZOII) in form of clear zone or area surrounding the tested films. This indicates that there is no inhibitory and bio-cidal properties of the films againts *E. coli*. From the analysis, chitosan used in this study had low degree of deacetylation, resulting in low positive charge density. In addition, tested chitosan composite films were not activated with water so that chemical bonds between gram negative bacteria and chitosan positive charges did not happen (Dehnad et al. 2015). In the view of chitosan/MFC nanocomoposite films, there was no opposite charge attractions between positive chitosan charges with negatively charged moieties of *E. coli* cell membrane. No interaction between chitosan and bacteria because of the formation of intermolecular and intramolecular hydrogen bonds between amine groups of chitosan and hydroxyl groups of MFC (Santos et al. 2014). In addition, the presence of amorphous part leading to self-aggregation will allow water to be penetrated in the chitosan/MFC nanocomposite films so that the microorganisms can grow and utilize the material as a source of energy.

Conclusion

MFC was successfully isolated by means of steam explosion assited with alkaline treatment. The thickness average of chitosan/MFC nanocomposite films varied. Different moisture content was presumably due to the existance of bound and free water interaction between hydroxyl groups of chitosan and MFC. The increase in MFC concentration induced irregular, unsmooth and uneven external surfaces of chitosan nanocomposite films due to non-homogenous distribution of the MFC. Some white-colored and aggerated spots were easily to be found with a size average of about 0.5 at MFC incorporation of 0.5–10%. No dramatic change was for C, O, and N observed in both neat chitosan and chitosan/MFC composite films but the reinforcement of MFC into chitosan slightly decreased the element of nitrogen. From FT-IR analysis, reinforcement of MFC altered IR wavenumber and intensity of chitosan/MFC nanocomposite films, indicating the chemical interaction between chitosan and MFC functional groups. There were

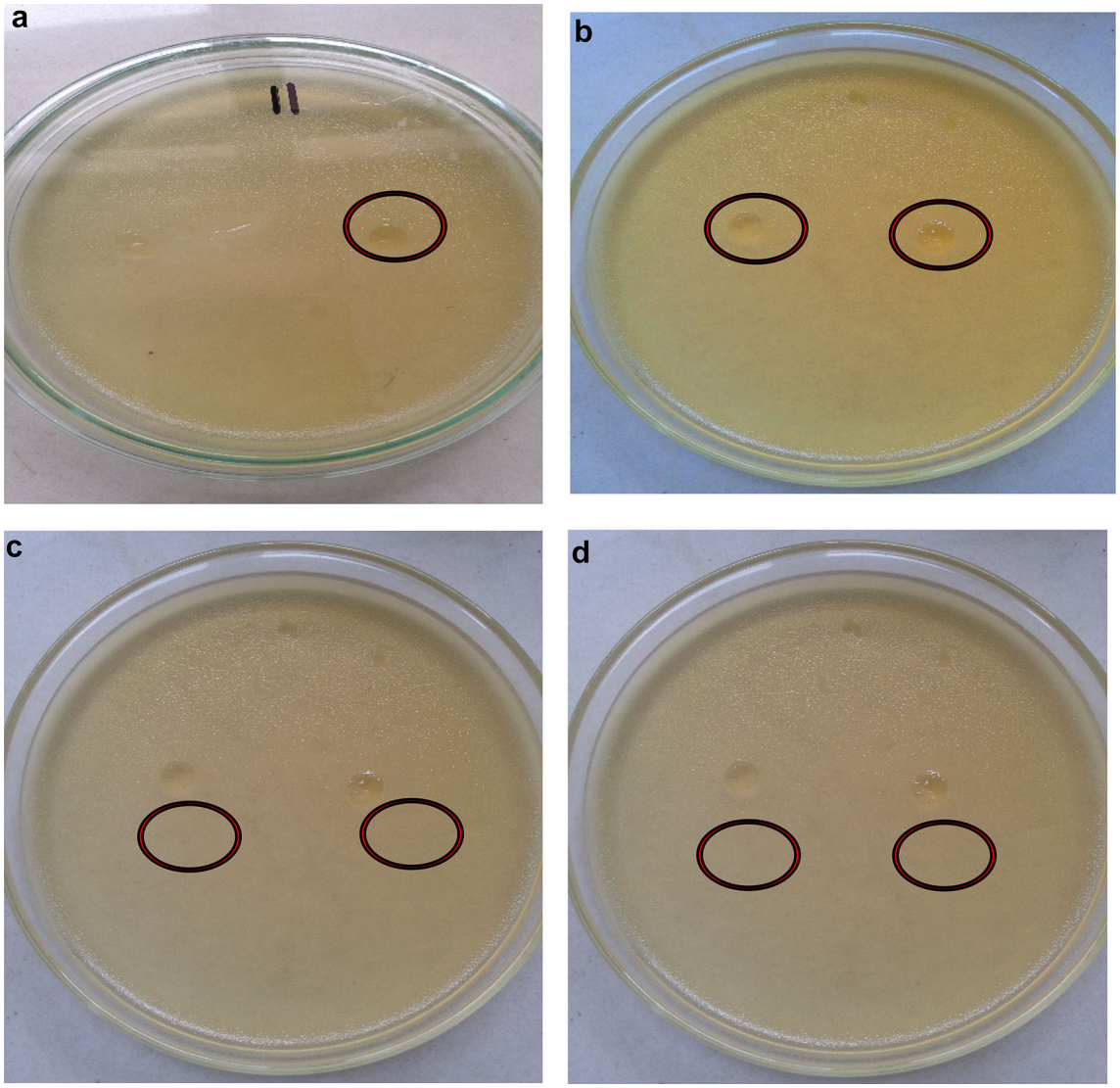

Fig. 8 Anti-bacteria properties of chitosan/MFCnanocomposite films **a** neat chitosan, **b** MFC 0.5%, and **c** MFC 2.5%, and **d** MFC 7.5%

two steps of thermal decomposition of the films, including water evaporation and structural degradation for both chitosan and MFC. The addition of MFC into chitosan polymer slowed the decomposition and degradation of the films due to the nucleating agent effects, and enhanced the thermal stabilities of chitosan/MFC through strong hydrogen bondings between MFC and chitosan polymer. No zone of inhibition (ZOI) in form of clear zone or area was found in the tested film (5 mm), indicating no inhibitory and bio-cidal properties of the films againts *E. coli*.

Acknowledgements We would like to sincere thank Directorate of Higher Education (DIKTI) of the Ministry of Research, Technology, and Higher Education (Menristekdikti RI) because of tremendous support for this research. We also acknowledge Department of Forest Products, Department of Physics, Department of Biology, and Department of Biochemistry of Bogor Agricultural University (IPB); Bandung Institute of Technology; and Shizuoka University for allowing us to conduct this study in their sites.

References

Azeredo HMC, Mattoso LHC, Bustillos RJA, Filho GC, Munford ML, Wood D, Mchugh TH (2010) Nanocellulose reinforced chitosan composite films as affected by nanofiller loading and plasticizer content. J Food Sci 75(1):1–7

Bajpai SK, Chand N, Ahuja S (2015) Investigation of curcumin release from chitosan/cellulose microcrystals (CMC) antimicrobial films. Int J Biol Macromol 79:440–448

Balan T, Guezennec C, Nicu R, Ciolacu F, Bobu E (2015) Improving barrier and strength properties of paper by multi-layer coating with bio-based additives. Cellulose Chem Technol 49:607–615

Caloch GR, Santes V, Escobar J, Romo PR, Diaz L, Rojas LL (2016) Effect of chitosan on the performance of NiMoP-supported catalysts for the hydrodesulfurization of dibenzothiophene. J Nanomater 2016:1–13

Celebi H, Kurt A (2015) Effects of processing on the properties of chitosan/cellulose nanocrystal films. Carbohydr Polym 133:284–293

Chang CW, Wang MJ (2013) Preparation of microfibrillated cellulose composites for sustained release of H_2O_2 or O_2 for biomedical applications. ACS Sustain Chem Eng 1:1129–1134

Charernsriwilaiwat N, Rojanarata T, Ngawhirunpat T, Opanasopit P (2012) Electrospun chitosan/polyvinyl alcohol nanofibre mats for wound healing. Int Wound J 11:215–222

Chen CH, Wang FY, Mao CF, Yang CH (2007) Studies of chitosan. I. Preparation and characterization of chitosan/poly(vinyl alcohol) blend films. J App Polym Sci 105:1086–1092

Cherian BM, Leao AL, De Souza SF, Thomas S, Pothan LA, Kotaisamy M (2012) Isolation of nanocellulose from pineapple leaf fibers by steam explosion. Carbohydr Polym 81:720–725

de Mesquita JP, Donnici CL, Texeira IF, Pereira FV (2012) Bio-based nanocomposites obtained through covalent linkage between chitosan and cellulose nanocrystals. Carbohydr Polym 90:210–217

Deepa B, Abraham E, Cherian BM, Bismarck A, Blaker JJ, Pothan LA, Leao AL, De Souza SF, Kottaisamy M (2011) Structure, morphology, and thermal characteristics of banana nano fibers obtained by steam explosion. Bioresour Technol 102:1988–1997

Dehnad D, Djomeh ZE, Mirzaei H, Jafari SM, Dadashi S (2015) Optimization of physical and mechanical properties for chitosan–nanocellulose biocomposites. Carbohydr Polym 105:222–228

Fernandes SCM, Freire CSR, Silvestre AJD, Neto CP, Gandini A, Berglund LA, Salmén L (2010) Transparent chitosan films reinforced with a high content of nanofibrillated cellulose. Carbohydr Polym 81:394–401

Goh KY, Ching YC, Chuah CH, Abdullah LC, Liou NS (2013) Individualization of microfibrillated celluloses from oil palm empty fruit bunch: comparative studies between acid hydrolysis and ammonium persulfate oxidation. Cellulose 23:379–390

Gulmen SST, Guvel EA, Kizilcan N (2015) Preparation and characterization of chitosan/polypyrrole/sepiolite nanocomposites. Procedia-Social Behav Sci 195:1625–1632

Haafiz MKM, Eichhorn SJ, Hassan A, Jawaid M (2013) Isolation and characterization of microcrystalline cellulose from oil palm biomass residue. Mater Let 113:87–89

Hafdani FN, Sadhegenia N (2011) A review on application of chitosan as a natural antimicrobial. Int J Med Health Biomed Bioeng Pharm Eng 5:46–50

Hassan MI, Hassan EA, Oksman KN (2011) Effect of pretreatment of baggase fibers on the properties of chitosan/microfibrillated cellulose nanocomposite. J Mater Sci 46:1732–1740

Herzele A, Veigel S, Liebner F, Zimmermann T, Altmutter WG (2015) Reinforcement of polycaprolactone with microfibrillated lignocellulose. Ind Crops Prod 93:255–266

Jabbour L, Gerbaldi J, Chaussy D, Zeno E, Bodoardo S, Beneventi D (2010) Microfibrillated cellulose–graphite nanocomposites for highly flexible paper-like Li-ion battery electrodes. J Mater Chem 20:7344–7347

Kumar V, Bollstrom R, Yang A, Chen Q, Chen G, Salminen P, Bousfield D, Toivakka M (2014) Comparision of nano- and microfibrillated cellulose films. Cellulose 21:3443–3456

Lewandowska K (2015) Characterization of chitosan composites with synthetic polymers and inorganic additives. Int J Biol Macromol 81:159–164

Li J, Wei X, Wang Q, Chen J, Chang G, Kong L, Su J, Liu Y (2012) Homogeneous isolation of nanocellulose from sugarcane bagasse by high pressure homogenization. Carbohydr Polym 90:1609–1613

Liu K, Lin X, Chen L, Huang L, Cao S, Wang H (2013) Preparation of microfibrillated cellulose/chitosan-benzalkonium chloride biocomposite for enhancing antibacterium and strength of sodium alginate films. J Agric Food Chem 61:6562–6567

Liu K, Lin X, Chen L, Huang L, Cao S (2014) Dual-function chitosan-methylisothiazolinone/microfibrillated cellulose biocomposite for enhancing antibacterial and mechanical properties of agar films. Cellulose 21:519–528

Mahmoudi N, Ostadhossein F, Simchi A (2016) Physicochemical and antibacterial properties of chitosan-pollyvinylpyrrolidone films containing self-organized graphene oxine nanolayers. J Appl Polym Sci 133:43194

Osong SH (2014) Mechanical pulp based nano-ligno-cellulose production, characterisation and their effect on paper properties, Master thesis, Mid Sweden University, Sundsvall, Sweden

Ostadhossein F, Mahmoudi N, Cid MG, Tamjid E, Martos FJN, Cuadrado BS, Paniza JML, Simchi A (2015) Development of chitosan/bacterial cellulose composite films containing nanodiamonds as a potential flexible platform for wound dressing. Materials 8:6401–6418

Paipitak K, Pornpra T, Mongkontalang P, Techitdheera W, Pecharapa W (2011) Characterization of PVA-chitosan nanofibers prepared by electrospinning. Procedia Eng 8:101–105

Pavaloiu RD, Guzun AS, Stroescu M, Jinga SI, Dobre T (2014) Composite films of poly(vinyl alcohol)-chitosan-bacterial cellulose for drug controlled release. Int J Biol Macromol 68:117–124

Postnova SS, Silant'ev V, Ha CS, Shchipunov Y (2015) Chitosan bionanocomposites prepared in the self-organized regime. Pure Appl Chem 87:793–803

Qi X, Yang G, Jing M, Fu Q, Chiu FC (2013) Microfibrillated cellulose reinforced bio-based poly(propylene carbonate) with dual shape memory and self-healing properties. J Mater Chem A 1–3:1–8

Romainor ABN, Chin SF, Pang SC, Bilung LM (2014) Preparation and characterization of chitosan nanoparticles-doped cellulose films with antimicrobial property. J Nanomater 2014:1–10

Santos C, Silva CJ, Buttel Z, Guimaraes R, Pereira SB, Tamagnini P, Zille A (2014) Preparation and characterization of polysaccharides/PVA blend nanofibrous membranes by electrospinning method. Carbohydr Polym 99:584–592

Siqueira G, Bras J, Dufresne A (2010) *Luffa cylindrica* as a lignocellulosic source of fiber, microfibrillated cellulose, and cellulose nanocrystals. BioResources 5:727–740

Solikhin A, Hadi YS, Massijaya MY, Nikmatin S (2017) Production of microfibrillated cellulose isolation by novel continuous steam explosion assisted chemo-mechanical methods and its characterizations. Waste Biomass Valoriz. https://doi.org/10.1007/s12649-017-0066-z

Solikhin A, Hadi YS, Massijaya MY, Nikmatin S (2018) Properties of poly(vinyl alcohol)/chitosan nanocomposite films reinforced with oil palm empty fruit bunch amorphous lignocellulose nanofibers. J Polym Envi. https://doi.org/10.1007/s10924-018-1215-6

Song K, Gao A, Cheng X, Xie K (2015) Preparation of the superhydrophobic nano-hybrid membrane containing carbon nanotube based on chitosan and its antibacterial activity. Carbohydr Polym 130:381–387

Tingaut P, Zimmerman T, Sebe G (2012) Cellulose nanocrystals and microfibrillated cellulose as building blocks for the design of hierarchical functional materials. J Mater Chem 22:20105–20111

Tome LC, Fernandes SCM, Perez DS, Sadocco P, Silvestre AJD, Neto CP, Marrucho IS, Freire CSR (2013) The role of nanocellulose fibers, starch and chitosan on multipolysaccharide based films. Cellulose 20:1807–1818

Wu T, Farnood R, O'Kelly K, Chen B (2014) Mechanical behavior of transparent nanofibrillar cellulose–chitosan nanocomposite films

in dry and wet conditions. J Mech Behav Biomed Mater 32:279–286

Zeid RAE, Hassan EA, Bettaieb F, Khiari R, Hassan M (2015) Use of cellulose and oxidized cellulose nanocrystals from olive stones in chitosan bionanocomposites. J Nanomater 2015:1–11

Zhou S, Wang M, Chen X, Xu F (2015) Facile tempelate synthesis of microfibrillated cellulose/polyprrole/silver nanoparticles hybrid aerogels with electrical conductive and pressure responsive properties. ACS Sustain Chem Eng 13:3346–3354